Influence of Association on Adsorption Properties of Block Copolymers

Boudewijn van Lent* and Jan M. H. M. Scheutjens

Department of Physical and Colloid Chemistry, Agricultural University, Dreijenplein 6, 6703 HB Wageningen, The Netherlands. *Received May 18, 1988; Revised Manuscript Received September 27, 1988*

ABSTRACT: The self-consistent field theory of Scheutjens and Fleer for the adsorption of homopolymers has been modified to study the adsorption of block copolymers from a selective solvent. With this extension it is possible to calculate the critical micelle concentration (cmc; for spherical or planar associates) and to show the influence of the self-aggregation of block copolymers on their adsorption behavior. The statistical weight of all possible conformations in the lattice is taken into account. Lateral interactions are calculated with a mean field approximation within each layer. For planar structures parallel lattice layers are used; for modeling micelles a spherical lattice is introduced. The cmc is determined from a small system thermodynamics argument of Hall and Pethica. For molecules with a long lyophobic block extremely low cmc values are found. The adsorption of these block copolymers on lyophobic surfaces increases sharply just below the cmc and is essentially constant at higher concentrations of polymer. Thick adsorption layers are formed. The effect of the interaction parameters is shown.

I. Introduction

Recently, the self-consistent field theory (SCF) of Scheutjens and Fleer[1,2] for homopolymer adsorption at the solid–liquid interface has been extended to the case of block copolymers.[3] This theory assumes equilibrium between adsorbed polymers and a homogeneous bulk solution. For homopolymers this assumption is reasonable for quite a large concentration range. Block copolymers, however, can form association structures like micelles and lamellar membranes. In that case the critical micelle (or membrane) concentration, the cmc, will limit the chemical potential of the polymer and, hence, the adsorption. When the cmc has been reached, polymer added to the solution will mainly aggregate and thus hardly affect the adsorption. For surfactants this has already been found experimentally; see for example ref 4 and 5.

Leermakers et al.[6] have derived equations to model chains in spherical and cylindrical lattices. Using these types of lattices, they have extended the SCF theory to calculate the equilibrium association structures for small surfactants. We will apply this method to investigate the association of block copolymers in solution and limit ourselves to spherical (micelle) and planar (membrane) lattices. The association structure with the lowest concentration of free polymer in solution and thus the lowest chemical potential is chosen as the equilibrium state. This concentration of free polymer is the maximum concentration for which calculation of the adsorption is relevant.

In this article the theories for the adsorption of block copolymers[3] and the association of surfactants[6] are combined. In section II we describe the SCF theory for block copolymers in associates of planar geometry. We shortly review the model for spherical micelles in section III. In section IV the calculation of the cmc is explained.

The influence of chain length and structure of the block copolymers on the cmc are shown in section V. We also examine the influence of the different interaction parameters. Finally, the adsorption behavior of these associating block copolymers is analyzed in some detail. Adsorption isotherms on lyophilic and lyophobic surfaces are shown. (We use the generic terms lyophilic and lyophobic for solvent-liking and solvent-disliking, respectively, to avoid less general terms like polar, apolar, hydrophilic, and hydrophobic.) The effects of chain length, block sizes, solvency, and adsorption energy on the adsorption are examined.

II. Self-Consistent Field Theory

In this section we explain the theory for a lattice of planar geometry. In case of adsorption at the solid–liquid interface the first lattice layer is assumed to be adjacent to the surface. For membranes the first layer is in the center of the bilayer, where a reflecting boundary is assumed. The layers are numbered $z = 1$ to M. Each layer has L sites. A lattice site has Z neighbors of which a fraction λ_1 is in the next, a fraction λ_0 in the same, and a fraction λ_{-1} in the previous layer. For a hexagonal lattice $\lambda_{-1} = \lambda_1 = 0.25$ and $\lambda_0 = 0.5$. A polymer or a solvent molecule of type i ($i = 1, 2, ...$) has a volume fraction $\phi_i(z)$ in layer z of which a volume fraction $\phi_{xi}(z)$ are segments of type x ($x = A, B, ...$). Similarly, $\phi_x(z)$ is the total volume fraction of x segments in layer z. So $\phi_x(z)$ is the summation of $\phi_{xi}(z)$ over all i, the total contribution from all molecules having segments of type x.

We neglect inhomogeneities within each layer z. Only the density profile perpendicular to the lattice layers will be considered. The SCF theory calculates the most probable set of conformations, where the system is at its minimum free energy. A conformation is defined as the sequence of layers in which the successive segments of a chain are situated.

For each segment s of molecule i we can write an end-segment distribution function $G_i(z,s|1)$. It describes the average weight of walks along molecule i, starting at segment 1 in an arbitrary layer in the system and ending after $s - 1$ steps in layer z. $G_i(z,s|1)$ is related to the end-segment distribution function of a walk of $s - 2$ steps ($s - 1$ segments):

$$G_i(z,s|1) = G_i(z,s)\{\lambda_{-1}G_i(z-1,s-1|1) + \lambda_0 G_i(z,s-1|1) + \lambda_1 G_i(z+1,s-1|1)\} \quad (1)$$

$G_i(z,s)$ is the statistical weight of a free segment s in layer z. If segment s is of type x then $G_i(z,s)$ equals the segment weighting factor $G_x(z)$. This is a Boltzmann factor, which gives the relative preference of segment type x to be in layer z rather than in the homogeneous bulk solution. In the bulk solution $G_x(z) = 1$. For every segment type one can define such a factor. The expression for these factors will be given later. Note that for copolymers each segment can be of a different type. Equation 1 is a recurrence relation. Starting with segment 1 and ending at segment r_i, we calculate all end-segment distribution functions of chains of lengths between 1 and r_i segments. For example,

0024-9297/89/2222-1931$01.50/0

if segment 1 is of type A we have $G_i(z,1|1) = G_A(z)$. When we consider adsorption, we set $G_x(z) = 0$ for $z \leq 0$. For membranes, however, we set $G_x(-z + 1) = G_x(z)$. This has the effect of placing a mirror between layers 0 and 1.

We want to know the distribution function $G_i(z,s|1;r)$ of segment s of a chain of r_i segments. We start a walk at segment 1 and another walk at segment r_i and stop both walks at segment s. $G_i(z,s|1;r)$ is a combination of end-segment distribution functions of the two walks:

$$G_i(z,s|1;r) = \frac{G_i(z,s|1)G_i(z,s|r)}{G_i(z,s)} \tag{2}$$

We divide by $G_i(z,s)$ because this factor is included in both walks. In this way we are able to calculate all the distribution functions of all segments. The sum of these functions gives the volume fraction $\phi_i(z)$ of molecules of given type i in layer z:

$$\phi_i(z) = C_i \sum_{s=1}^{r} \frac{G_i(z,s|1)G_i(z,s|r)}{G_i(z,s)} \tag{3}$$

One can find $\phi_{Ai}(z)$ by performing the summation in eq 3 only over those segments that are of type A. The quantity C_i is a normalization factor. We can derive this factor from the volume fraction ϕ_i^b in the bulk solution, where all the end-segment distribution functions are unity. If we substitute this into eq 3, we see that

$$C_i = \phi_i^b / r_i \tag{4}$$

We can also express C_i in the total amount $\theta_i = \sum_z \phi_i(z)$ of polymer segments in the system (in equivalent monolayers). The average of the end-segment distribution function of a chain of r_i segments is $\sum_{z=1}^{M} G_i(z,r|1)/M$. The average volume fraction equals θ_i/M. Hence

$$C_i = \frac{\theta_i}{r_i \sum_{z=1}^{M} G_i(z,r|1)} \tag{5}$$

As said before, to use eq 1, we need an expression for $G_A(z)$, $G_B(z)$, etc. The molecules will distribute themselves according to the effective potential field they are feeling. The energy of a certain conformation is the sum of the potentials $u(z)$ of the different segments. A molecule of three segments with segment A in layer 1 and two B segments in layer 2 would have an energy level of $u_A(1) + 2u_B(2)$. The weighting factor for this conformation would be $\lambda_1\lambda_0 \exp((-u_A(1) - 2u_B(2))/kT)$. This should be equal to $\lambda_1\lambda_0 G_A G_B^2$. The segmental weighting factor $G_x(z)$ is now defined as

$$G_x(z) = \exp(-u_x(z)/kT) \tag{6}$$

The expression for $u_x(z)$ has been derived from statistical thermodynamics.[3]

$$u_x(z) = u'(z) + kT \sum_y \chi_{xy}(\langle \phi_y(z) \rangle - \phi_y^b) \tag{7}$$

The subscripts x and y can refer to any segment in the system (A, B, ...). The site volume fraction, $\langle \phi_x(z) \rangle$, is defined as

$$\langle \phi_x(z) \rangle = \lambda_{-1}\phi_x(z - 1) + \lambda_0\phi_x(z) + \lambda_1\phi_x(z + 1) \tag{8}$$

In eq 7, the first term, $u'(z)$, is a potential that accounts for the hard-core interaction in layer z relative to the bulk solution and is independent of the segment type. It is essentially a Lagrange multiplier, which arises in the free energy minimization[3] because of the boundary condition $\sum_i \phi_i(z) = 1$. Physically, with increasing segment density, the hard-core potential (with respect to the bulk solution) is assumed to switch from $-\infty$ to $+\infty$ at the moment that $\sum_i \phi_i(z)$ passes 1. The equilibrium values of $u'(z)$ depend strongly on the system under consideration and are of the order of 1 kT or less. Unfortunately, no explicit expression for $u'(z)$ is available. The values are obtained by numerically adjusting $u'(z)$ so that $\sum_i \phi_i(z)$ (obtained from eq 3) is unity for each layer z.

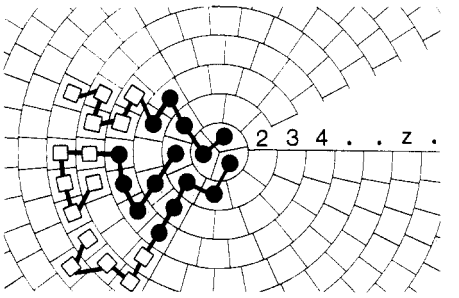

Figure 1. Block copolymers in a spherical lattice.

The second part of eq 7 expresses the specific interaction term, in which χ_{xy} is the familiar Flory–Huggins parameter for the interaction between monomers of types x and y.[7] For z large $\phi_x(z) = \phi_x^b$, $u_x(z) = 0$, and $G_x(z) = 1$. In the summation over y, we have also included the interaction energy between a segment and the surface (x = S). The volume fraction of the solid is 1 in layer 0 and 0 for $z >$ 0. As we can see from eq 7 the interaction between segments A and the surface S equals $\chi_{AS}\lambda_1$.

With eq 3, 6, and 7 and the condition that $\sum_i \phi_i(z) = 1$ for each layer z, we are in principle able to calculate numerically the adsorption profile or the profile of a membrane for a given amount of polymer or a given bulk concentration.[1,3]

III. Spherical Lattices

By comparing calculated free energies of membranes and micelles, we can analyze which structure is preferred. For the modeling of micelles we have to modify the structure of the lattice. Figure 1 shows a cross section through the center of a spherical lattice. The layers are numbered sequentially, starting at the center of the lattice. For the spherical lattice the following conditions must hold: 1. All lattice sites have equal volume. 2. All lattice layers are equidistant. 3. The coordination number Z is constant for each lattice site.

These conditions have certain consequences. Sites in different layers have different shapes. The total number of lattice sites $L(z)$ in layer z is no longer an integer. The position of neighboring sites is variable. The volume $V(z)$ in number of lattice sites of a spherical lattice equals

$$V(z) = (4/3)\pi z^3 \tag{9}$$

Differentiating eq 9 with respect to z gives the surface area:

$$S(z) = 4\pi z^2 \tag{10}$$

The number of sites in layer z is the difference in volume between $V(z)$ and $V(z - 1)$:

$$L(z) = V(z) - V(z - 1) \tag{11}$$

In the spherical lattice, λ_0, λ_1, and λ_{-1} are functions of z. The following relation must still hold:

$$\lambda_{-1}(z) + \lambda_0(z) + \lambda_1(z) = 1 \tag{12}$$

If we generate a particular conformation of a molecule and calculate its statistical weight, it should not make any difference at which end of the molecule we have started our walk. Therefore

$$Z\lambda_{-1}(z)L(z) = Z\lambda_1(z - 1)L(z - 1) \tag{13}$$

The transition factors λ_{-1} and λ_1 are proportional to the surface area per site in contact with the adjacent layer. Thus, the final equations are given by

$$\lambda_1(z) = \lambda_1^{b}S(z)/L(z) \qquad \lambda_{-1}(z) = \lambda_{-1}^{b}S(z-1)/L(z) \quad (14)$$

where λ_1^{b} and λ_{-1}^{b} are the values of the transition factors for the equivalent planar lattice, i.e., at $z \to \infty$. For micelles the λ's in eq 1 and 8 have to be substituted by those of eq 12 and 14. In eq 5, θ_i has to be replaced by $n_i r_i$, which equals $\sum_{z=1}^{M} L(z)\phi_i(z)$, and the denominator changes into $r_i \sum_{z=1}^{M} L(z)G_i(z,r|1)$.

IV. The Cmc

The theory for association structures as outlined in sections II and III gives us the equilibrium structure of a single micelle or membrane in equilibrium with a homogeneous bulk solution. What we do want to know is the critical micelle or (membrane) concentration of a solution of block copolymers, where an unknown number of micelles is being formed. In this section the equilibrium condition for a micellar solution is explained and the implementation of this condition into our model is described.

We can apply small system thermodynamics to our micellar solution.[8] The solution is divided into subsystems of a volume V_s, which contain one micelle each and have a composition that is determined by the overall concentration $\bar{\phi}_i$. The excess free energy A_s^{exc} of a small system can be defined. It contains a part A_m^{σ}, which describes the free energy necessary to create a micelle with fixed center of mass and an entropy term which contains the translational entropy of the micelles.[8]

$$A_s^{exc} = A_m^{\sigma} + kT \ln(V_m/V_s) \quad (15)$$

V_m is the volume of a micelle. The expression for A_m^{σ} is equivalent with the expression for the surface free energy in ref 3:

$$A_m^{\sigma}/kT = -\sum_z L(z)u'(z) - \sum_i n_i^{exc}$$

$$-\tfrac{1}{2}\sum_x\sum_y\sum_z L(z)\chi_{xy}\{\phi_x(z)\langle\phi_y(z)\rangle - \phi_x^{b}\phi_y^{b}\} \quad (16)$$

A typical curve for A_m^{σ} as a function of n_2^{exc}, the excess number of molecules 2 aggregated in a spherical micelle with respect to their equilibrium concentration, is shown in Figure 2a. This figure is calculated with the theory as outlined in the previous sections for a system consisting of $A_{70}B_{30}$ molecules (component 2) in a B solvent (component 1), with $\chi_{AB} = 1$. Throughout this paper, the A block is lyophobic. With increasing n_2^{exc}, the free energy A_m^{σ} initially rises, as it is unfavorable for the molecules to aggregate in such small numbers. The interaction energy gained is outweighted by the loss in entropy of the individual molecules. Above a certain aggregation number, in this case 18, it becomes energetically more and more favorable to associate and A_m^{σ} decreases. In equilibrium[8]

$$dA = -S\,dT - P\,dV + \sum \mu_i\,dn_i + A_s^{exc}\,dN_m = 0 \quad (17)$$

where A is the free energy of the whole system of volume $V = N_m V_s$ and N_m is the total number of micelles (or subsystems). To fulfill the condition that $dA = 0$ at constant T, V, and $\{n_i\}$, A_s^{exc} has to be zero. If A_s^{exc} would be negative or positive, A would decrease by forming a higher or lower number of micelles, respectively. Applying this to eq 15 shows that the extra free energy due to aggregation must be balanced by the entropy of the micelles. Moreover, from eq 15 we see that A_m^{σ} should be positive, because obviously $V_m \leq V_s$.

We will now derive how the equilibrium concentration ϕ_2^{b} of polymer depends on the composition $\bar{\phi}_2$ of the system. The excess number of polymer molecules n_2^{exc} in micelles is related to the small system volume V_s, expressed in number of lattice sites, and the overall composition $\bar{\phi}_2$ by $n_2^{exc}r_2 = V_s(\bar{\phi}_2 - \phi_2^{b})$. Rewriting this relation gives

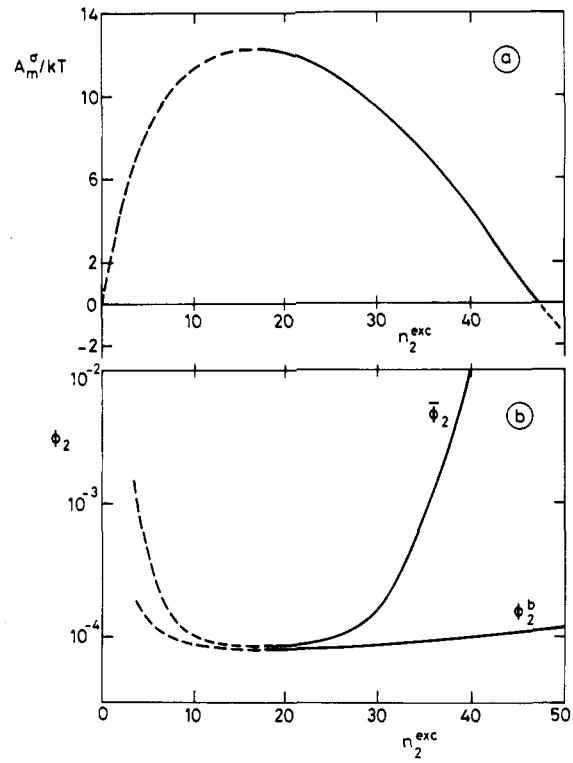

Figure 2. (a) Excess free energy of aggregation A_m^{σ}, as a function of the excess number of $A_{70}B_{30}$ molecules per micelle, n_2^{exc}, in a B solvent. (b) Corresponding composition $\bar{\phi}_2$ and the equilibrium polymer concentration ϕ_2^{b} in the same system. The dashed part of the curves represent thermodynamically unstable regimes. $\chi_{AB} = 1$.

$$V_s = \frac{n_2^{exc}r_2}{\bar{\phi}_2 - \phi_2^{b}} \quad (18)$$

As the volume fraction of polymer in the core of a micelle is virtually constant, the volume of a micelle expressed in number of lattice sites can be approximated by

$$V_m \approx \frac{n_2^{exc}r_2}{\phi_2(1) - \phi_2^{b}} \quad (19)$$

Combination of eq 15, 18, and 19 gives

$$\bar{\phi}_2 \approx (\phi_2(1) - \phi_2^{b})e^{-A_m^{\sigma}/kT} + \phi_2^{b} \quad (20)$$

allowing $\bar{\phi}_2$ to be computed from the concentration profile. In Figure 2b, $\bar{\phi}_2$ and ϕ_2^{b} are plotted as a function of n_2^{exc}. It can be seen that a minimum concentration, the cmc, is necessary to create micelles. Note that, in correspondence with the Gibbs adsorption equation, ϕ_2^{b} is at its minimum when A_m^{σ} is at its maximum. Increasing the composition beyond the cmc will increase n_2^{exc}. For the same composition, ϕ_2^{b} at the right-hand side of the minimum, and therefore the chemical potential, μ_2, is lower than the corresponding value at the left-hand side. Therefore, the dashed portion of the curves in Figure 2 represent thermodynamically unstable micelles. In Figure 3, the overall composition $\bar{\phi}_2$ is subdivided into the equilibrium concentration, ϕ_2^{b}, and the excess volume fraction of aggregated molecules, $\bar{\phi}_2 - \phi_2^{b}$. At the cmc, the equilibrium concentration ϕ_2^{b} drops because of the formation of micelles. The concentration of micelles and hence the reduction in equilibrium concentration equals the difference

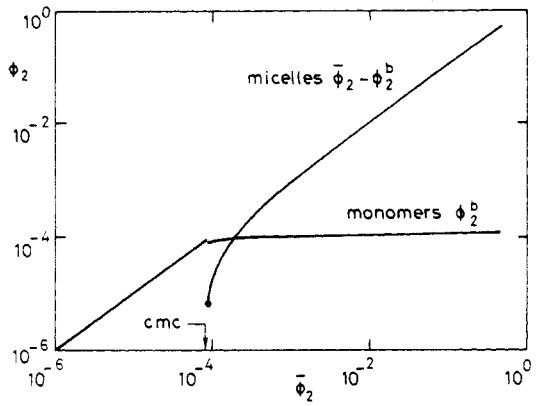

Figure 3. Equilibrium concentration ϕ_2^b and volume fraction of micelles $\bar{\phi}_2 - \phi_2^b$ as a function of composition $\bar{\phi}_2$ for an $A_{70}B_{30}$ block copolymer in a B solvent.

between the two curves at their minimum (around $n_2^{exc} = 18$) in Figure 2a. It can be seen that beyond the cmc the equilibrium concentration hardly increases and all additional molecules aggregate, as expected.

The procedure for calculating the equilibrium concentration for a given composition $\bar{\phi}_2$ is as follows. We start with a certain number n_i of each molecule in a system of M layers. With the theory, as outlined in sections II and III, n_i^{exc} and ϕ_i^b are calculated. Substitution of these parameters and the chosen composition into eq 18 and 19 gives the small system and micelle volumes. Substituting these values and A_m^σ, obtained from eq 16, into eq 15 gives A_s^{exc}. Now the amount of polymer in the M layers can be changed and the whole procedure can be repeated until $A_s^{exc} = 0$. Obviously, a numerical procedure is needed to solve this problem. Note that the small system volume may be different from the volume of the M layers under consideration.

For membranes, L is very large and the entropy term per surface site $L^{-1} \ln (V_m/V_s)$ is negligible. We only have to find the equilibrium concentration ϕ_2^b for which A_m^σ/L equals zero.

V. Results and Discussion

In the first part of this section some general trends for micelle and membrane formation will be studied. In the second part the influence of micellization on the adsorption of block copolymers will be shown. For all the calculations λ_1^b and λ_{-1}^b have been taken equal to 0.25 (hexagonal lattice). The choice of lattice slightly affects the numerical results but not the general trends; see for example ref 1, 9, and 10.

In Figure 4, typical segment density profiles are shown of a micelle of $A_{70}B_{30}$ block copolymers in a B solvent. The interaction between A and B segments is repulsive: $\chi_{AB} = 1$. In the center of the micelle a high concentration of A segments is found. This concentration is essentially equal to that in the concentrated phase at the binodal, calculated with Flory's equation for phase separation between an A_{70} homopolymer and a B solvent.[7] The core of A segments is surrounded by a shell of B segments, where the solvent density is not much lower than in the bulk solution. The concentration of solvent in the core is far from zero. For higher values of χ_{AB} this concentration decreases strongly.

In Figure 5, the effect of the number of lyophobic segments on the formation of micelles and membranes is shown for an AB block copolymer of 100 segments in a B solvent. In this figure $\chi_{AB} = 1.5$. The concentration where global phase separation between solvent and polymer would occur has also been calculated, using the extended

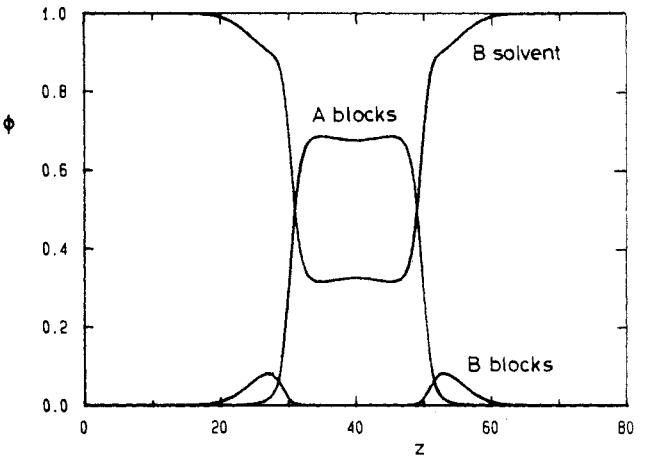

Figure 4. Segment density profiles of a micelle of an $A_{70}B_{30}$ block copolymer in a B solvent. The layers are renumbered; $z = 40$ is the center of the micelle. $\chi_{AB} = 1$.

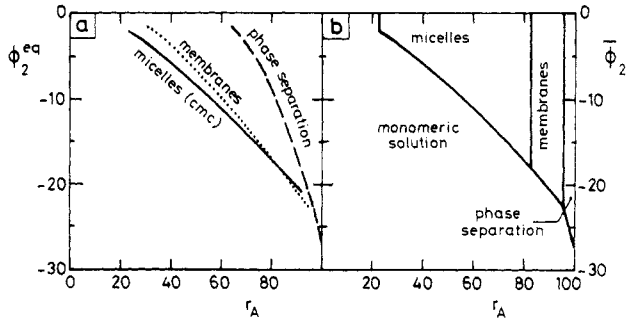

Figure 5. Phase behavior of AB block copolymers of chain length $r_2 = 100$ in a B solvent. $\chi_{AB} = 1.5$. (a) Equilibrium concentration of polymer in the presence of micelles (solid curve), membranes (dotted curve), and global phase separation (dashed curve) as a function of the number of A segments per molecule. (b) Phase diagram, in which the regions are indicated where micelles, membranes, phase separation, and a monomeric solution occur.

Flory–Huggins formulas for the chemical potential μ_i of (randomly mixed) copolymers.[3]

$$(\mu_i - \mu_i^*)/kT = \ln(\phi_i) + 1 - r_i \sum_j \phi_j/r_j + (1/2) r_i \sum_x \sum_y \chi_{xy}(\phi_{xi}^* - \phi_x)(\phi_y - \phi_{yi}^*) \quad (21)$$

Here, μ_i^* is the chemical potential and $\phi_{xi}^* = r_{xi}/r_i$ is the volume fraction of segments of type x, in amorphous polymer of type i. A more detailed analysis of the phase behavior of random copolymers has been made by Koningsveld and Kleintjes.[11] In Figure 5a, the equilibrium concentration for micelles, membranes, and global phase separation is shown as a function of r_A. As is known from Figure 2, for micelles this concentration varies only slightly with composition. For (noninteracting) membranes and phase separation this concentration is independent of $\bar{\phi}_2$. If the A blocks are very short, there is no aggregation. Micelles are formed if the length of the A block is long enough. The critical micelle concentration is lower than the critical membrane concentration, except for high A/B ratios. When the B part becomes much smaller than the A part, a transition from micellar- to membrane-like structures (with a smaller surface area per molecule) is found. Finally, when the polymers consist mainly of A segments, the polymer and solvent will phase separate globally, because χ_{AB} is larger than the critical value for homopolymers of 100 A segments. The cmc for block copolymers with a large fraction of A is extremely low. This means that these molecules will usually be associated. Lowering χ_{AB} or decreasing the molecular weight will in-

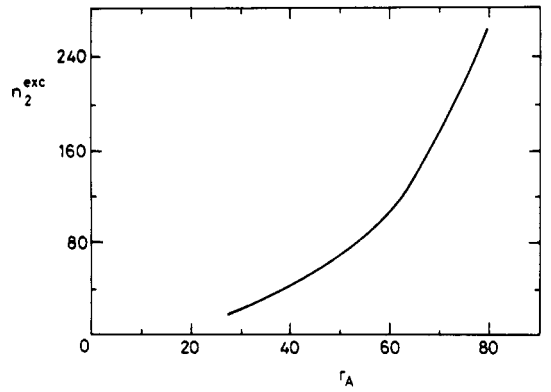

Figure 6. Aggregation number n_2^{exc} of a micelle as a function of the number of A segments in the polymer of Figure 5.

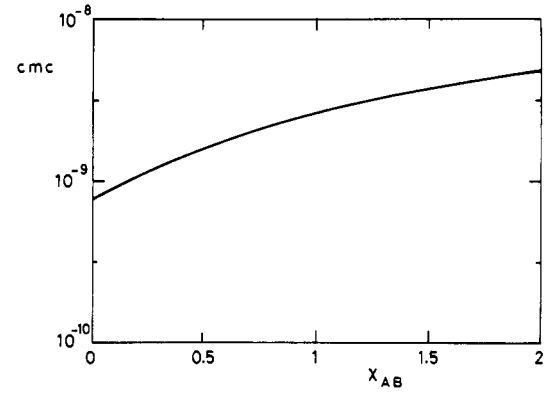

Figure 7. Critical micelle concentration of an $A_{50}B_{50}$ diblock copolymer as a function of χ_{AB}. The χ parameters for the segment solvent interactions are $\chi_{AO} = 1.5$ and $\chi_{BO} = 0$.

crease the cmc, which is mainly a function of $r_A\chi_{AB}$. In Figure 5b a phase diagram is constructed by plotting $\bar{\phi}_2$ instead of ϕ_2^b. The areas where micelles, membranes, phase separation, and a monomeric solution occur are indicated. In this case, the lines form the boundaries between the different regions where the various structures exist. On the boundary between micelles and membranes both association structures coexist, i.e. they have the same equilibrium concentration for a certain composition. Here, this transition is rather sharp and virtually independent of $\bar{\phi}_2$, but in other systems there could be a wider range of coexistence. Of course, other structures than spherical or lamellar aggregates are possible, but these examples illustrate clearly a well-known transition from more spherical to more lamellar structures as the A/B ratio increases.

In Figure 6, the aggregation number n_2^{exc}, of micelles of AB diblock copolymers from Figure 5, is plotted as a function of the length of the A block. As expected, the aggregation number increases strongly with increasing length of the A block.

The interaction between A and B segments is usually independent of the solvent quality. In Figure 5, the solvent molecules are of the same type as the B segments in the polymer. In Figure 7, the interaction χ_{AB} between the two segment types of an $A_{50}B_{50}$ block copolymer is varied, while the interactions between A and B segments and solvent (O) is kept constant ($\chi_{AO} = 1.5$ and $\chi_{BO} = 0$). A lower χ_{AB} appears to decrease the cmc. In the micelle are more contacts between A and B blocks than in the homogeneous bulk solution. Therefore, a higher χ_{AB} is unfavorable for aggregation. At $\chi_{AB} = 1.5$ the situation as in Figure 5 at $r_A = 50$ is recovered.

In Figure 8a, adsorption isotherms are shown for three different diblock copolymers, differing in A/B ratio: $A_{70}B_{30}$, $A_{50}B_{50}$, and $A_{30}B_{70}$. The A segments adsorb preferentially, $\chi_{AS} = -4$, while $\chi_{BS} = 0$. The interaction parameters between the different monomers are the same as in Figure 5. The adsorption isotherms are plotted as a function of the overall composition of the solution. For the $A_{30}B_{70}$ block copolymers the adsorbed amount increases steadily until the cmc at $\bar{\phi}_2 = 26 \times 10^{-5}$ is reached. The adsorption hardly increases any further, because the concentration of free polymer in solution remains almost constant. The adsorption levels off near the point where A_m^σ is maximal (see Figure 2). The $A_{70}B_{30}$ and $A_{50}B_{50}$ molecules show a slightly different behavior. An S-shaped isotherm can be observed: as soon as a few chains adsorb, a cooperative aggregation effect of A segments on the surface occurs. The adsorbed amount of the $A_{70}B_{30}$ increases until a semiplateau is reached. Near the cmc, θ_2^{exc} rises again very sharply and levels off at the cmc. Adsorption isotherms with similar shape have been found for small surfactant molecules; see for example ref 4 and 5. The surface acts as a condensation nucleus.

In parts b–d of Figure 8 the segment density profiles of the three different polymers at their maximum adsorbed amount are shown. The surface is occupied by A segments, whereas the B blocks form dangling tails. The longer the B block the further the polymer extends into the solution. Eventually, the densities of A and B segments decrease exponentially to their solution concentration. The dip in the profile of segments A in Figure 8d occurs because these segments try to avoid the thick unfavorable layer of B segments.

Figure 9 illustrates the effect of chain length on the

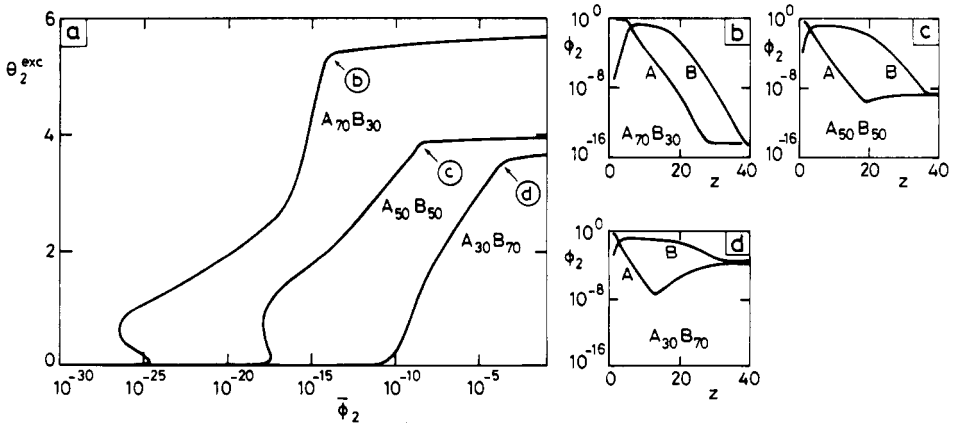

Figure 8. (a) Adsorption isotherms for three different block copolymers $A_{70}B_{30}$, $A_{50}B_{50}$, and $A_{30}B_{70}$ in a B solvent. Segment density profiles calculated in the plateau region of the adsorption isotherms: (b) $A_{70}B_{30}$, $\phi_2^b = 7 \times 10^{-15}$, $\theta_2 = 5.4$; (c) $A_{50}B_{50}$, $\phi_2^b = 26 \times 10^{-10}$, $\theta_2 = 3.9$; (d) $A_{30}B_{70}$, $\phi_2^b = 26 \times 10^{-5}$, $\theta_2 = 3.6$. Interaction parameters: $\chi_{AB} = 1.5$, $\chi_{AS} = -4$, $\chi_{BS} = \chi_{OS} = 0$.

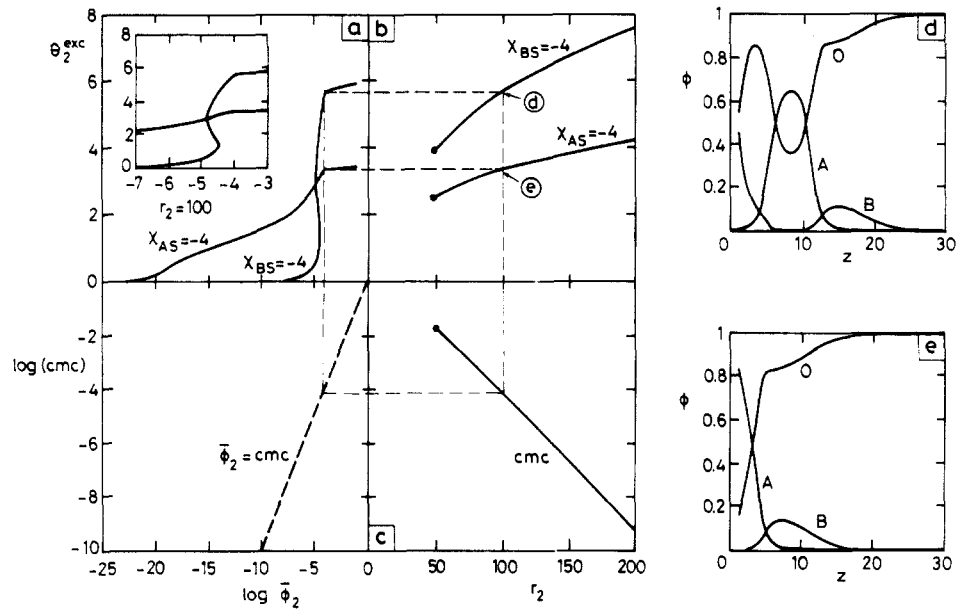

Figure 9. Relation (dashed lines) between adsorption isotherms (a and inset), the adsorption at the cmc (b) and the cmc as a function of the chain length (c), both for adsorbing A segments ($\chi_{AS} = -4$, $\chi_{BS} = 0$) and for adsorbing B segments ($\chi_{AS} = 0$, $\chi_{BS} = -4$). Segment density profiles at the points indicated in b are given in d and e. $r_A/r_2 = 0.7$, $\chi_{AB} = \chi_{AO} = 1$, $\chi_{BO} = 0$.

adsorbed amount and the difference in adsorption between molecules with adsorbing A blocks and molecules with adsorbing B blocks. In all the graphs of Figure 9, we have used $r_A/r_2 = 0.7$, $\chi_{AB} = \chi_{AO} = 1$ and $\chi_{BO} = 0$. In Figure 9a, adsorption isotherms are shown for $r_2 = 100$. The curve for adsorbing A blocks ($\chi_{AS} = -4$) can be compared with the $A_{70}B_{30}$ curve in Figure 8a, where $\chi_{AB} = 1.5$ instead of 1. Now the adsorption starts at about the same equilibrium concentration, but the cooperative effect has disappeared and the cmc is much higher for these molecules. The cooperative effect reappears when $\chi_{BS} = -4$ (adsorbing lyophilic blocks). This is more evident in the inset of Figure 9a. The volume fraction at which adsorption starts is much higher in this case, because the B blocks are much shorter than the A blocks. In Figure 9b, the excess adsorbed amount, θ_2^{exc}, at the cmc is shown as a function of chain length r_2. For the upper curve $\chi_{BS} = -4$, while $\chi_{AS} = \chi_{OS} = 0$, for the lower curve $\chi_{AS} = -4$ and $\chi_{BS} = \chi_{OS} = 0$. The concomitant cmc values are plotted in Figure 9c. The adsorbed amount is about twice as much when B rather than A segments adsorb preferentially. When $\chi_{BS} = -4$, a bilayer is formed at the surface. This is illustrated in Figure 9d, where a segment density profile for $r_2 = 100$ has been drawn. The B segments have a maximum in their profile in the layer adjacent to the surface and a second smaller maximum about 15 layers away from the surface. The A segments have a maximum in their profile at $z = 8$, while the concentration of solvent is minimal at this distance. In Figure 9e a profile is shown for the case that $\chi_{AS} = -4$ and $r_2 = 100$. Here, only a monolayer is formed. Although the cmc reduces drastically when r_2 is increased (Figure 9c), in both cases the adsorbed amount still rises with increasing chain length (Figure 9b). The dashed lines in Figure 9 connect points for the same situation (at the cmc for $r_2 = 100$) and have been drawn to show the relation between parts a–c of Figure 9. The bottom left quadrant has no physical relevance.

In Figure 10, the excess adsorbed amount at the cmc is shown as a function of the adsorption energy of A blocks, χ_{AS}, for $A_{30}B_{70}$ and $A_{50}B_{50}$ molecules in a B solvent. As in Figure 8, $\chi_{AB} = 1.5$ and $\chi_{BS} = 0$. The adsorbed amount of $A_{30}B_{70}$ molecules increases strongly when χ_{AS} becomes more negative than a critical value. This is also well-known

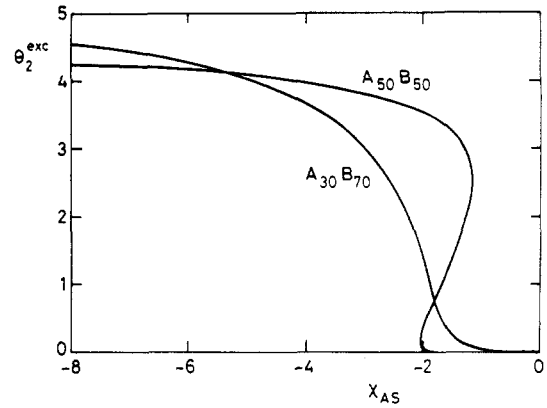

Figure 10. Excess adsorbed amount calculated at the cmc as a function of χ_{AS} for $A_{30}B_{70}$ (cmc = 26×10^{-5}) and $A_{50}B_{50}$ (cmc = 26×10^{-10}) molecules in a B solvent. $\chi_{AB} = 1.5$ and $\chi_{BS} = 0$.

from adsorption of homopolymers.[12,13] The $A_{50}B_{50}$ molecules show an S-shaped curve. This arises from the cooperative adsorption of these molecules (see also Figure 8). The S-shape in Figure 10 occurs only if the S-shape in the adsorption isotherm (such as in Figure 8a) is located around the cmc and χ_{AS} is near the critical value.

VI. Conclusions

The length of lyophobic A blocks in combination with the solvent quality ($r_A\chi_{AO}$) is the leading factor for the critical micelle concentration of diblock copolymers. A strong repulsion between A and B segments (high χ_{AB}) slightly opposes aggregation. Usually the aggregates are spherical, but when the lyphobic A blocks are much longer than the B blocks, a lamellar bilayer (membrane) is the preferred aggregation structure, because of its smaller surface area per molecule. The concentration of solvent in the lyophobic center of the aggregates can be high.

Aggregation of block copolymers influences the adsorption properties of these molecules strongly. Beyond the cmc the adsorption on a solid–liquid interface is almost constant. When the lyophobic block adsorbs preferentially and is much longer than the lyophilic block, a strong increase in the adsorbed amount occurs near the cmc. If the solvent quality is extremely poor (high χ_{AO}), the cmc is very

low, an S-shaped isotherm can be observed, and the adsorbed amount in the plateau region is high. Clearly, the surface acts as a condensation nucleus. Reducing the length of the A block or increasing the solvent quality raises the cmc and diminishes the S-shape of the isotherm. Competition between adsorption and micellization is observed only for weakly adsorbing A blocks in a very poor solvent. If the lyophilic block adsorbs on a lyophilic surface, a bilayer can be formed on the surface.

References and Notes

(1) Scheutjens, J. M. H. M.; Fleer, G. J. *J. Phys. Chem.* **1979**, *83*, 1619.
(2) Scheutjens, J. M. H. M.; Fleer, G. J. *J. Phys. Chem.* **1980**, *84*, 178.
(3) Evers, O. A. Thesis, Wageningen Agricultural University, 1989.
(4) Mathai, K. G.; Ottewill, R. H. *Trans Faraday Soc.* **1966**, *62*, 750; *Ibid.* 759.
(5) Corkhill, J. M.; Goodman, J. F.; Tate, J. R. *Trans Faraday Soc.* **1966**, *62*, 979.
(6) Leermakers, F. A. M.; Van der Schoot, P. P. A. M.; Scheutjens, J. M. H. M.; Lyklema, J. In *Surfactants in Solution, Modern Applications*; Mittal, K. L., Ed.; in press.
(7) Flory, P. J. *Principles of Polymer Chemistry*; Cornell University Press: Ithaca, NY, 1953.
(8) Hall, D. G.; Pethica, B. A. In *Nonionic Surfactants*; Schick, M. J., Ed., Marcel Dekker: New York, 1976; Chapter 16.
(9) Roe, R. J. *J. Chem. Phys.* **1974**, *60*, 4192.
(10) Cosgrove, T.; Heath, T.; Van Lent, B.; Leermakers, F.; Scheutjans, J. *Macromolecules* **1987**, *20*, 1692.
(11) Koningsveld, R.; Kleintjes, L. *Macromolecules* **1985**, *18*, 243.
(12) Scheutjens, J. M. H. M.; Fleer, G. J.; Cohen Stuart, M. A. *Colloids Surf.* **1986**, *21*, 285.
(13) Van der Beek, G. P.; Cohen Stuart, M. A. *J. Physique (Les Ulis, Fr.)* **1988**, *49*, 1449.

Effects of Entropic Barriers on Polymer Dynamics

M. Muthukumar*

Polymer Science and Engineering Department, University of Massachusetts, Amherst, Massachusetts 01003

A. Baumgärtner

Institut fur Festkorperforschung der Kernforschungsanlage Julich, Postfach 1913, D-5170 Julich, Federal Republic of Germany.

Received January 28, 1988; Revised Manuscript Received September 23, 1988

ABSTRACT: Dynamic and static properties of a self-avoiding polymer chain in an infinite periodic array of cubic cavities separated by short bottlenecks have been investigated by Monte Carlo simulations and analyzed by scaling arguments. At the locations of the bottlenecks, entropic barriers are set up due to the reduction of the number of possible chain configurations in these positions. Consequently the chain diffusion coefficient D is smaller than the Rouse diffusion coefficient D_0. The scaling analysis of the effect of entropic barriers shows that D/D_0 decays exponentially with chain length N if the cross section of the bottleneck C is large and that it is independent of N for small C but is now a function of C, according to $N^{-1} \ln (D/D_0) = A - sN^{-1}$ where s depends inversely on C and A depends inversely on the size of the cavity and is negative. The simulation results are in agreement with the scaling analysis demonstrating that the chain diffusion in this problem is dominantly controlled by the entropic barriers.

I. Introduction

Diffusion of polymer chains in random media controls a wide variety of phenomena such as exclusion chromatography, membrane separations, ultrafiltration, viscoelasticity of polymer solutions, etc. In view of this, extensive literature exists on the experimental results on porous media, membranes, and polymer solutions dealing with these phenomena.[1-10]

The fundamental issue in these problems is the transport of a polymer chain from a region of larger volume where the chain entropy is higher to another region of smaller volume where the chain entropy is lower. Thus the polymer chain moves across an entropic barrier. Since the experimental situations are typically very complex and many factors contribute to the observed phenomena, it is desirable to perform computer simulations on a well-characterized model system in order to understand the effects of entropic barriers on polymer dynamics. Such an effort is the main focus here.

In this paper we study the effects of entropic barriers on chain diffusion by following Monte Carlo simulations of the escape of a self-avoiding chain from a well-characterized cubic cavity through the gates (bottlenecks or capillaries) at the centers of the walls of the cavity (cf. Figure 1). We have actually considered an infinite three-dimensional periodic array of such cavities with each cavity containing six bottlenecks. By changing the chain length N and the size C of the bottlenecks we have monitored the chain diffusion coefficient D and its dependence on N and C.

Whenever the chain transports from a region of large volume to another region of small volume, the monomer concentration is partitioned[11-14] between these two regions due to the differences in chain entropy in different confining spaces. The diffusion coefficient of the chain is determined by the partition coefficient which is the ratio of the monomer concentration in the capillary to that in the cavity. The partition coefficient was first calculated by Casassa[11] for Gaussian chains. This calculation was later generalized by Daoud and de Gennes[12,13] and Brochard and de Gennes[14] using scaling arguments for good solutions. These scaling predictions have been verified by Guillot et al.[7] by an experimental investigation of diffusion of large flexible chains through model membranes.

Since the length of the bottlenecks is very short in the model considered here, the scaling arguments[12-14] of de Gennes and co-workers must be accordingly modified. The consideration of small length of bottlenecks in the present study is motivated by the presence of bottlenecks in the

0024-9297/89/2222-1937$01.50/0